Resonance Raman Spectra of Metallooctaethylporphyrins. A Structural Probe of Metal Displacement

L. D. Spaulding, C. C. Chang, Nai-Teng Yu,* and R. H. Felton*

Contribution from the School of Chemistry, Georgia Institute of Technology, Atlanta, Georgia 30332. *Received September 10, 1974*

Abstract: Comparison of resonance Raman spectra of D_{4h} and D_{2d} molecular forms of octaethylporphinatonickel(II) (NiOEP) indicates high-frequency bands at 1660, 1609, 1581, and 1524 cm^{-1} are structure-sensitive. Upon deuteration at the meso carbons two additional anomalously polarized bands appear with a concomitant decrease in intensity of the 1310-cm^{-1} anomalously polarized line. The spectrum in solution is consistent with a planar NiOEP structure. Spectra of CuOEP imply the existence of two molecular forms in this compound. An empirical correlation between the position of the anomalously polarized line at ~1590 cm^{-1} and the distance from the center of the porphyrin ring to the pyrrole nitrogen is applied to hemeprotein resonance Raman data. It is inferred that out-of-plane displacements of the iron atom are 0.4 Å in deoxyhemoglobin and 0.3 Å in fluoromethemoglobin.

The application of resonance Raman spectroscopy to biological[1-6] systems is an area of intense activity. The utility of this technique as a structural probe of the chromophore in hemeproteins has stimulated several studies[7-11] on protein-free porphyrins and metalloporphyrins. Empirical correlations between the positions of Raman lines and the metal oxidation state or metal-to-porphyrin plane distances exemplify some of the information accessible by resonance Raman spectroscopy. Also, the appearance or shift of lines permits identification of peripheral substituents, and the dependence of the depolarization ratio of certain lines as the wavelength of the incident radiation varies is interpreted as evidence for electronic symmetry reduction.

In a preliminary communication[11] we reported on the structure-sensitive 1590-cm^{-1} line and suggested that the frequency of this line indicated whether the metal was in-plane or out-of-plane. In the present work a more detailed examination of the influence of the porphyrin structure on the resonance Raman spectrum is reported. It is found that the above interpretation to be generally correct but, as anticipated from a consideration of the scattering process, must be modified to reflect directly a property of the porphinato core. From a study of metallooctaethylporphyrins (MOEP) it is possible to demonstrate an empirical correlation between the ~1590-cm^{-1} frequency and the distance from the center of the porphyrin core to the pyrrole nitrogen atoms. By examining tetragonal and triclinic crystals of NiOEP in which the molecular symmetry is D_{2d}[12] and D_{4h},[13] respectively, a direct influence of structure on the resonance Raman spectrum is demonstrated.

Experimental Section

Raman spectra were determined using a Spex 1401 double monochromator, Coherent Radiation Model 52G argon-ion laser, and photon-counting electronics. Spectra were obtained using 0.5–1.0 m*M* solution of the porphyrin dissolved in either CH_2Cl_2 or H_2O, in KBr pellets (0.5 mg of porphyrin/200 mg of KBr), or as a crystalline powder affixed to transparent tape. There were no differences in the spectra determined on the tape and in KBr pellets; however, low laser power levels must be used on the crystalline samples to avoid decomposition. Spectra were taken with 514.5-, 488.0-, and 457.9-nm irradiation. A rotating cell or platform was used to prevent photodecomposition of the porphyrin during laser irradiation. Peak positions are accurate to 2 cm^{-1}. The depolarization ratio is $\rho = I_\perp/I_\parallel$, where $I_\perp$ and $I_\parallel$ are the intensities of light scattered, respectively, perpendicular and parallel to the incident polarization.

Materials. Dichloromethane was distilled from CaH_2 and stored over molecular sieves. Other solvents, gases, and chemicals were the highest quality available commercially and were not further purified.

Octaethylporphyrin, H_2OEP, was generously supplied by Professors D. Dolphin and J. H. Fuhrhop. The Fe(III), Mn(III), Co(II), Ni, Cu, VO, and Zn complexes were synthesized by conventional techniques[14] and purified by chromatography and recrystallization. Their electronic absorption spectra agree with published spectra. The Sn(IV) complex was prepared using Dolphin's procedure,[15] and the Zn porphyrin was obtained via Fuhrhop's preparation.[16] An aqueous solution of the protoporphyrin IX iron(III) ligated by cyanide[17] was prepared at pH 10.8 with a large excess of ligand. An optical spectrum of the solution agreed with the published spectrum. The protoporphyrin IX iron(II) complexes were formed[18] by addition of excess dithionite to aqueous solutions of the ligated ferric porphyrin. A solution of pyridine protoporphyrin IX iron(II) was prepared at pH 6.8 by solubilizing the porphyrin with 3% sodium dodecylsulfate. $Fe^{II}OEP(L)_2$, L = imidazole or pyridine, were synthesized by a procedure of Kobayashi.[19] $Co^{III}OEPX$, $X^- = Br^-$ or ClO_4^-, were obtained by bromine oxidation or electrolysis.[20]

Samples of the two crystal forms of NiOEP were obtained with the conditions reported by Cullen and Meyer;[12,13] however, the preparation of the tetragonal form was contaminated with triclinic crystals. The long needles, characteristic of the triclinic crystal, were removed manually. Triclinic crystals were prepared with hexane–dichloromethane solutions. Densities of the crystals agree with reported values.

Octaethylporphyrin-*meso*-d_4. This compound was prepared[21] from H_2OEP-h_4 by exchange in D_2SO_4–D_2O. After one exchange a minimum of 94% deuterium incorporation at the meso carbons was observed (^1H NMR spectrum).

Octaethylporphinato-*meso*-d_4-nickel(II). The nickel was inserted in pyridine solvent. Following metal insertion, the solution was added to water and NiOEP extracted into CH_2Cl_2. The solution was washed five times with water, dried over Na_2SO_4, and filtered, and NiOEP crystallized from a CH_2Cl_2–hexane solution. The crystals were dried in vacuo at 150°. Deuterium incorporation at the meso carbons was 1 (d_1), 4 (d_2), 9 (d_3), and 86% (d_4).

Chlorooctaethylporphinato-*meso*-d_4-iron(III). Synthesis is the same as for the nickel compound, except DMF was employed as solvent. Deuterium incorporation was 92% (mass spectrum).

Nitrosyletioporphyrinatocobalt. NO was bubbled slowly for 10 min into a $CHCl_3$ solution of cobaltous etioporphyrin I. Stirring was continued for an additional 30 min under the NO atmosphere. Argon was bubbled through the solution to remove excess NO, methanol was added, and after 2 days dark purple crystals were formed. The crystals were filtered and washed with methanol: ir (KBr) 1665 cm^{-1} (NO). Anal. Calcd for $C_{32}H_{36}CoN_5O$: C, 69.94; H, 6.56; N, 12.75. Found: C, 69.75; H, 6.23; N, 12.62.

Nitrosyloctaethylporphyrinatoiron. To a solution containing 20 mg of $Fe^{III}OEPCl$, 12 ml of $CHCl_3$, and 6 ml of CH_3OH, 50 mg of $NaBH_4$ was added. NO was bubbled slowly through the solution for 15 min. The solution was stirred under the NO atmosphere for 1 hr. The solution was filtered and reduced in volume to about 5 ml on a steam bath, and 20 ml of CH_3OH was added. After cooling, the dark purple crystals appearing were filtered and air-dried giv-

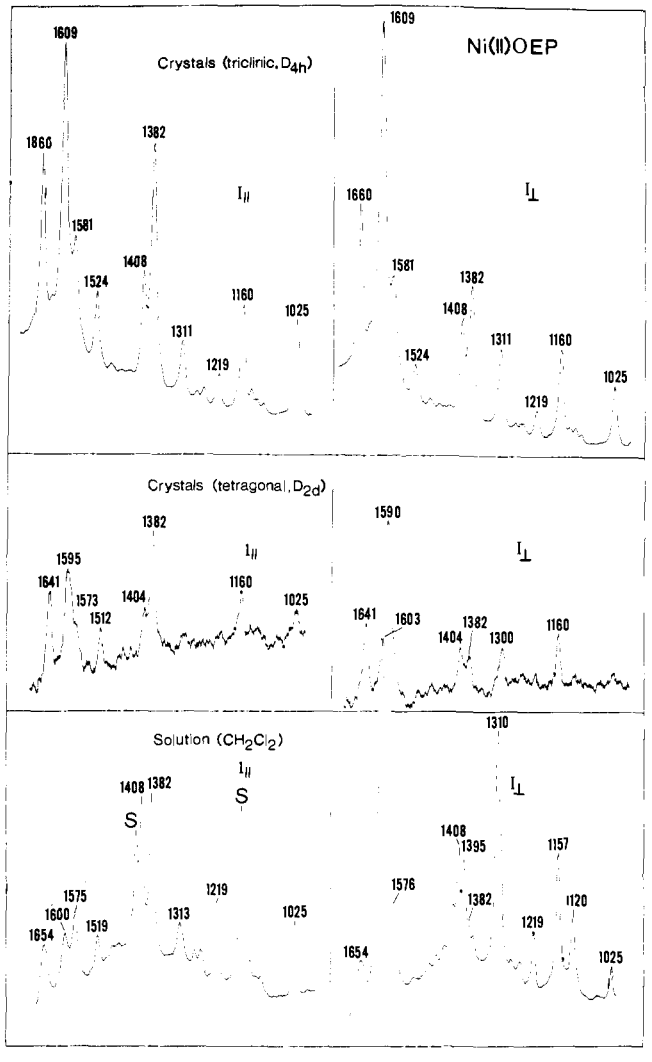

Figure 1. Resonance Raman spectra of crystalline and solution samples of NiOEP-h_4 (irradiated at 514.5 nm).

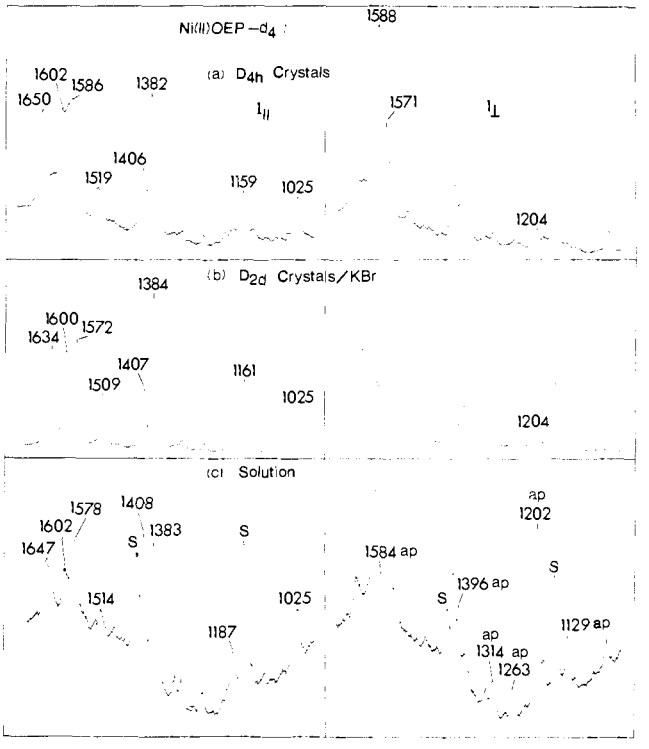

Figure 2. Resonance Raman spectra of crystalline and solution samples of NiOEP-d_4 (irradiated at 514.5 nm).

ing 12 mg (60%): ir (KBr) 1671 cm^{-1} (NO). Anal. Calcd for $C_{36}H_{44}FeN_5O$: C, 69.90; H, 7.12; N, 11.32. Found: C, 69.80; H, 7.00; N, 10.02.

Octaethylporphyrinatocarbonylpyridineiron(II). A mixture of 40 mg of $Fe^{III}OEPCl$, 6 ml of CH_3OH, 1.2 ml of pyridine, and 12 ml of $CHCl_3$ was refluxed under an argon stream for 20 min. Then 50 mg of $NaBH_4$ was added and refluxing continued under a slow stream of CO. After 3 hr, 25 ml of CH_3OH saturated with CO was added and the solvent removed by distillation. When the temperature reached 60°, 25 ml of CH_3OH saturated with CO was added. The solution was cooled in an ice bath and filtered, and the purple crystals were washed with CH_3OH and air-dried on the filter yielding 35 mg (85%): ir (KBr) 1962 cm^{-1} (CO). Anal. Calcd for $C_{42}H_{49}FeN_5O$: C, 72.50; H, 7.10; N, 10.07. Found: C, 72.81; H, 7.49; N, 9.62.

Results

Spectra of the triclinic and tetragonal crystal forms of NiOEP-*meso*-h_4 together with the CH_2Cl_2 solution spectrum are shown in Figure 1. Either crystal form when dissolved resulted in identical solution spectra. Reduced laser power levels must be employed during recording of the crystal spectra. The tetragonal form, containing a molecule of nitromethane, was particularly sensitive to degradation; the reduced power used is responsible for the decreased S/N ratio shown in the spectrum. Similar spectral features are displayed in Figure 2 for crystalline and solution sample spectra of NiOEP-*meso*-d_4. Comparison of spectra of the triclinic crystals as a crystalline powder or embedded in a KBr matrix shows no difference in peak positions. Prolonged grinding of the tetragonal form will cause partial conversion to the triclinic form as demonstrated by band shifts in the spectrum.

In Table I, peak maxima and a qualitative assessment of depolarization ratios, ρ, are tabulated for the NiOEP's. Polarized lines (p) have $\rho < 3/4$, depolarized lines (dp) have $\rho = 3/4$, and anomalously polarized (ap) lines are characterized by $\rho > 3/4$.

Enhancement of polarized line intensity by irradiation at 457.9 nm with concomitant diminishment of dp and ap line intensity aids in the assignments listed and establishes in solution spectra the presence of overlapping bands at 1600 and 1310 cm^{-1}. Identification of lines is greatly aided by examination of the NiOEP-d_4 spectra in which, for example, a shift of the 1603 (ap) cm^{-1} band present in the NiOEP-h_4 solution spectrum exposes clearly an underlying 1602 (p) cm^{-1} peak.

Besides band shifts, deuteration at the meso carbons induces (1) the appearance of two new anomalously polarized bands in addition to the four ap bands commonly observed and (2) intensity changes in the ap bands. New ap bands are noted at 1263 and 1202 cm^{-1} with the latter appearing prominently in the $I_{\perp}$ spectrum. A striking decrease in $I_{\perp}$ intensity is seen in the 1313-cm^{-1} (ap) vibration. These changes are noted also in the FeOEPCl-d_4 spectrum (Table II).

In Figure 3 the resonance Raman spectra are given of (a) CuOEP crystals embedded in a KBr pellet obtained from D. Dolphin, (b) CuOEP crystals prepared from CH_2Cl_2–hexane solution, and (c) a solution spectrum of CuOEP. The same solution spectrum was obtained with either CuOEP preparation. Also, the spectrum shown in Figure 3a was observed when the same crystal sample was irradiated without the KBr support. The most striking feature is the multiplicity of lines shown in Figure 3a when compared to the simpler crystalline or solution spectrum. By analogy to the spectral shifts observed in the NiOEP spectra, we conclude that CuOEP sample supplied by D. Dolphin is a mix-

Table I. Resonance Raman Spectra of NiOEP[a]

NiOEP triclinic (D_{4h})		NiOEP tetragonal (D_{2d})		NiOEP soln (CH_2Cl_2)	
H	D	H	D	H	D
1660 (s, dp)	1650 (s, dp)	1641 (s, dp)	1634 (s, dp)	1654 (s, dp)	1647 (s, dp)
	1602 (s, ?p)	1595 (s, p)	1600 (s, p)	1600 (s, p)	1602 (s, p)
1609 (s, ap)	1588 (s, ap)	1590 (s, ap)	1571 (s, ap)	1603 (s, ap)	1584 (s, ap)
1581 (m, dp)	1586 (s, ?)	1573 (m, dp)	1572 (s, dp)	1575 (s, dp)	1578 (s, dp)
1524 (m, p)	1519 (m, p)	1512 (m, p)	1509 (m, p)	1519 (m, p)	1514 (m, p)
1491 (w, dp)				1480 (w, dp)	1480 (w)
				1466 (w, dp)	
1408 (m, dp)	1406 (m, dp)	1404 (m, dp)	1407 (m, dp)	1408 (s, dp)	1408 (s, dp)
			1393 (w, ap)	1395 (s, ap)	1396 (s, ap)
1382 (s, p)	1382 (s, p)	1382 (s, p)	1384 (s, p)	1382 (s, p)	1383 (s, p)
	1334 (w)		1334 (w)	1313 (m)	1329 (m, dp)
1311 (m, ap)	1312 (w, ap)	1311* (m, ap)	1312 (w, ap)	1310 (s, ap)	1314 (m, ap)
1274 (w, dp)		1274* (w, dp)		1276 (w, dp)	
1258 (w, dp)	1259 (w)	1258* (w, dp)	1260 (w)	1260 (w, dp)	1263 (m, ap)
1219 (w, dp)		1218* (w, dp)		1219 (s, dp)	
	1202 (w, ap)		1204 (w, ap)		1202 (s, ap)
	1184 (w, dp)		1185 (w, dp)		1187 (m, dp)
1160 (m, dp)	1159 (m, dp)	1160 (m, dp)	1161 (m, dp)	~1160 (overlapped with a solvent band)	~1160
1139 (w, p)	1136 (w, p)	1138* (w, p)	1139 (w, p)	1140 (w, p)	1141 (w, p)
1124 (w, ap)	1127 (w, ap)			1120 (s, ap)	1129 (s, ap)
1108 (w)	1109 (w)	1107* (w)	1109 (w)	1110 (w)	1111 (w)
1025 (m, p)	1025 (m, p)	1025 (m, p)	1025 (m, p)	1025 (s, p)	1025 (s, p)
958* (w)	959 (w)	964* (w)	965 (w)		
		943* (w)			
904* (w)		899* (w)			
		844* (w)			
802* (w)	769 (w)	803* (w)	798 (w)	Masked by solvent	
	773 (w)	774* (w)	773 (w)		
		761* (w)	763 (w)		
749* (w)	755 (w)	749* (w)			
673* (w)	686 (w)	673* (w)	680 (w)		
	668 (w)	609* (w)	667 (w)		
		551* (w)			
		526* (w)			
		481* (w)			
353* (w)	349 (w)	352* (w)	348 (w)		
276* (w)	274 (w)	283* (w)			
			242 (w)		
225* (w)	236 (w)	243* (w)	219 (w)		

[a] Spectra were taken with crystalline samples excepting lines marked by an asterisk; these were measured with a sample in KBr support.

ture containing two molecular forms of CuOEP. We have been unable in this laboratory to prepare a sample which exhibits the 1660 (dp), 1605 (ap), and 1513 (p) cm^{-1} bands. That a simple solution spectrum is found when this sample is dissolved obviates impurity contamination.

Generally, the spectra of the metalloporphyrins were taken with KBr pellets for uniformity of comparison and to reduce the fluorescence background of complexes containing a closed-shell metal. Exceptions are four iron protoporphyrin IX complexes which were examined in aqueous solution and low-spin iron(II) complexes. The latter were prepared by reduction of a CH_2Cl_2 solution of the ferric form with methanolic $NaBH_4$ or aqueous sodium dithionite solutions. Manipulations were carried out in an oxygen-free environment.

Discussion

Description of the Scattering Process. Peticolas' theory[4,22] of Raman scattering yields the following expression for the scattering tensor near resonance.

$$\alpha_{ij} = \sum_{\mu,\lambda} \frac{M_{\mu g}{}^{i}\left\langle \mu \left| \left(\frac{\partial H}{\partial \xi}\right)_0 \right| \lambda \right\rangle M_{g\lambda}{}^{j}\langle \mathbf{1} | \xi | 0 \rangle}{(\nu_\mu + \Omega - \nu + i\tau)(\nu_\lambda - \nu + i\tau)} \quad (1)$$

Here $M_{\mu g}{}^{i}$ is the electronic dipole moment element along $i = x,y,z$ for transitions from the ground electronic state g to an excited electronic state μ; ν_μ and ν_λ are the excitation frequencies to the excited states μ and λ; ν and Ω are the incident photon and vibrational frequencies, respectively. τ is a damping constant. Vibronic coupling between excited states is effected by the operator $(\partial H/\partial \xi)_0$ with ξ the vibrational coordinate. The matrix element $\langle 1|\xi|0\rangle$ is the vibrational transition moment in the ground state g.

In metalloporphyrins with D_{4h} molecular symmetry the excited states are E_u symmetry.[23] The medium intensity, visible Q bands and intense B (Soret) band characterizing the electronic absorption spectra arise from configuration interaction.

Vibrations of a_{1g}, a_{2g}, b_{1g}, or b_{2g} symmetry can appear in the resonance Raman spectrum corresponding, respectively, to polarized, inversely polarized ($\rho = \infty$), and depolarized lines. The increase in intensity of a_{1g} (polarized) modes as ν increases toward ν_B is ascribed[4] to the $\mu = \lambda = B$ state term in eq 1. However, appearance of the remaining vibrations requires a mixing sequence, $\mu \neq \lambda$. Their intensity is maximized when the factors in the denominator of eq 1 are each at a minimum, that is, when ν is at a frequency of the 0–0 or 0–1 electronic transition. Predicted maxima are observed in hemeprotein[24] and in nickel or copper mesoporphyrin IX dimethyl ester spectra[10] upon irradiation of the Q band. Reference to the symmetry indicators of McClain[25] shows that lowering of molecular symmetry from D_{4h} to D_{2d} will not induce mixing of the antisymmetric tensor component with the isotropic or symmetric components. Thus, classification of a line as polarized, depolarized, or anomalously

Table II. Resonance Raman Spectra of FeOEPCl and CuOEP

Fe^{III}OEPCl (KBr)		Fe^{III}OEPCl soln (CH_2Cl_2)			
H	D	H	D	CuOEP crystal	CuOEP soln (CH_2Cl_2)
1630 (s, dp)	1620 (s, dp)	1632 (s, dp)	1620 (s, dp)	1638 (s, dp)	1638 (s, dp)
~1585 (s, p)	1585 (m, ?)			1593 (s, p)	1591 (s, p)
1568 (s, ap)	1552 (s, ap)	1567 (s, ap)	1553 (s, ap)	1585 (s, ap)	1584 (s, ap)
1562 (s, dp)	1560 (s, dp)	1561 (m, dp)	1560 (s, dp)	1569 (s, dp)	1570 (s, dp)
1486 (m, p)	1523 (w, p)	1473 (?)		1505 (m, p)	1504 (m, p)
	1457 (w, dp)				
1454 (m, p)					
1407 (s, dp)	1403 (s, dp)	1407 (s, dp)	1406 (s, dp)	1405 (m, dp)	1406 (s, dp)
1393 (m, ap)	1393 (m, ap)	1394 (m, ap)	1394 (w, ap)		1395 (w, ap)
1378 (s, p)	1375 (s, p)	1376 (s, p)	1376 (s, p)	1379 (s, p)	1379 (s, p)
1312 (s, ap)	1313 (m, ap)	1308 (s, ap)	1315 (w, ap)	1316 (m, ?)	1316 (s, ap)
				1279 (w, p)	1262 (m, p)
	1267 (w, ap)		1267 (w, ap)		
1214 (m, dp)		1213 (m, dp)		1213 (w, dp)	1208 (w, dp)
	1203 (s, ap)		1204 (w, ap)		
	1189 (w, dp)		1189 (w, dp)		
1160 (s, dp)	1158 (s, dp)	1159 (s, dp)	1159 (s, dp)	1162 (m, dp)	~1160 (masked by CH_2Cl_2)
1141 (m, p)	1139 (w, p)			1138 (m, p)	1137 (w, p)
1126 (m, ap)	1129 (w, ap)	1126 (w, ap)	1130 (w, ap)		
1028 (m, p)	1028 (s, p)	1028 (w, p)	1030 (m, p)	1025 (m, p)	1025 (m, p)
964 (m, p)	965 (w, p)				
937 (w, p)	935 (w)			958 (w)	
812 (w)		Masked by solvent		805 (w)	Masked by solvent
786 (w)	783 (w)			767 (w)	
752 (m, p)				751 (w)	
736 (w)					
676 (w)	686 (w)			679 (m)	
354 (m, p)	353 (w, p)			358 (w)	
	310 (w)			322 (w)	
274 (w)				274 (w)	
220 (w)	233 (w)			232 (w)	

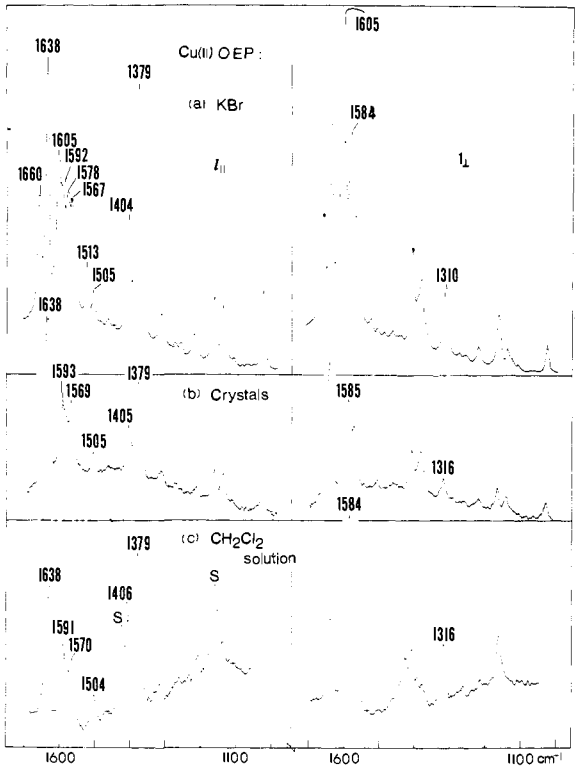

Figure 3. Resonance Raman spectra of CuOEP (irradiated at 514.5 nm): (a) sample supplied by D. Dolphin; (b) sample obtained from CH_2Cl_2–hexane solution; (c) CH_2Cl_2 solution sample of a or b.

polarized is valid in D_{2d} symmetry. The term anomalously polarized (ap) has been introduced to indicate an appreciable $I_\parallel$ component in a line which has $I_\perp > I_\parallel$. The $I_\parallel$ component for an ap line may be due to accidental degeneracy of an inversely polarized line with a depolarized or polarized vibration or, in cases of low molecular symmetry, mixing of the scattering tensor components.[26]

Nickel and Copper Porphyrins. Comparison of the recently reported[10] resonance Raman spectrum of nickel mesoporphyrin IX dimethyl ester with NiOEP (D_{4h} solution) shows close correspondence for the majority of observed lines; this result is anticipated since all β-pyrrole carbon atoms are substituted by alkyl or effectively alkyl groups (propionic acid ester). A shift of ca. 4 cm^{-1} in the peak maxima of solution spectra of the two nickel compounds is ascribed to the differing solvents employed: carbon disulfide and methylene dichloride. The present results, however, point to an unresolved component at 1313 cm^{-1} which overlaps with the 1310 (ap) cm^{-1} line used previously as an example[10,27] for which dispersion in ρ was interpreted in terms of reduced molecular symmetry. The 5-cm^{-1} shift observed in CH_2Cl_2 solution spectra (Figure 4) of nickel etioporphyrin I clearly indicates structure in this band. The observed behavior of ρ increasing to a maximum as ν passes through the Q 0–0 and 0–1 bands, then decreasing as ν falls between ν_Q and ν_B could be equally as well explained by accidentally degenerate polarized or depolarized and inversely polarized lines. In the earlier studies this possibility was noted, but no evidence was found of two components in 1310–1313-cm^{-1} line. Since the spectral pattern observed in solution indicates D_{4h} symmetry for NiOEP (vide infra), we doubt that wavelength dependence of ρ for this band implies lowering of electronic symmetry.

By altering the structure of NiOEP (Table III) it is possible to identify those resonance Raman bands which display frequency shifts. Reference to Table I yields the observation that the high-frequency bands are structure-sensitive; in the NiOEP-h_4 complex of D_{4h} molecular symmetry the 1660-, 1609-, 1581-, and 1524-cm^{-1} lines are shifted to 1641, 1590, 1573, and 1512 cm^{-1}, respectively, in the D_{2d} form. Similar shifts are noted in the NiOEP-d_4 complexes. Below 1500 cm^{-1}, with the possible exception of the 958-cm^{-1} band, lines are not structure-sensitive.

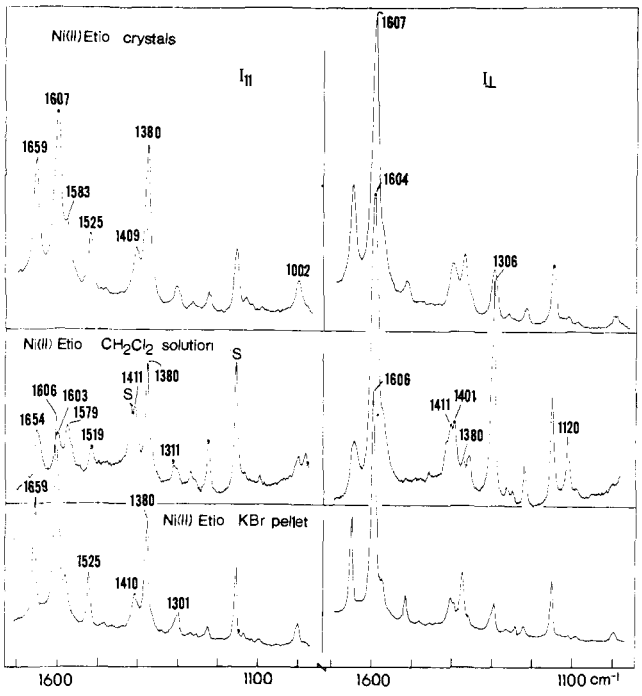

Figure 4. Resonance Raman spectra of etioporphyrin I nickel(II) (irradiated at 514.5 nm): (a) crystalline sample; (b) CH_2Cl_2 solution sample; (c) crystals in KBr support.

Table III. Average Bond Lengths (Å) in Nickel Porphyrins

Bond	NiOEP,[a] D_{2d}	NiOEP,[b] D_{4h}
Ni–N	1.929 (3)	1.958 (2)
C_a–N	1.386 (2)	1.376 (6)
C_a–C_m	1.372 (2)	1.371 (4)
C_a–C_b	1.449 (5)	1.443 (3)
C_b–C_b	1.362 (5)	1.346 (2)

[a] Reference 12; averaged, chemically equivalent bonds. [b] Reference 13. [c] Figures in parentheses are root mean square standard deviation of the average. Numerical value refers to least significant figure.

Preliminary results of a normal coordinate analysis of NiOEP (D_{4h}) by Abe, Kitagawa, and Kyogoku,[28] using the force constants of Ogoshi et al.,[29] indicate that with the exception of the a_{1g} vibration, the high-frequency modes shown in Table IV share a common feature of possessing a total of ~60–80% contribution from ν (C_a–C_m) and ν (C_a–N) or δ (C_aC_bN) where C_m is the methine carbon and C_a and C_b are, respectively, the α- and β-carbon atoms of pyrrole. (See Figure 5 for the labeling scheme of MOEP.) The 1660 (dp) and 1609 (ap) cm^{-1} lines which display the greatest shift contain the largest percentage of ν (C_a–C_m), ~70%. The bands are shifted by 19 cm^{-1} to lower frequencies in the D_{2d} molecular form. On the other hand, the 1602 (p) cm^{-1} of NiOEP-d_4 contains reduced amounts of ν (C_a–C_m) (~15%) or ν (C_a–N) and is not structure-sensitive.

The contribution of ν (C_a–C_m) to the a_{2g} vibration has been noted earlier[1] and with inclusion of ν (C_a–N) or δ (C_bC_aN) contributions stresses the importance of the inner 16-membered ring of metalloporphyrins.[30] Presumably, changes in the relevant force constants rather than kinematic effects dominate the observed shifts. Hoard's analysis[31] of metalloporphyrin stereochemistry lends credence to a view that structural changes in the porphinato core due to retention of planar pyrrole units will modulate the geometry of the 16-membered inner ring and thus induce vibrational frequency shifts. In the present instance S_4 ruffling is the structural modification of the porphinato ring which yields Raman shifts; however, evidence is adduced later which implies that expansion of the 16-membered ring will also lower the Raman frequencies.

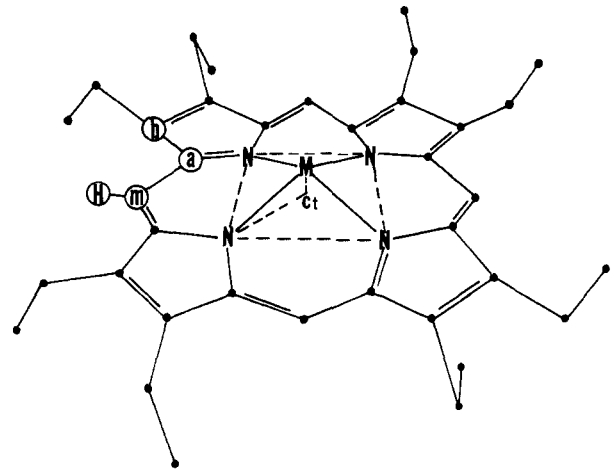

Figure 5. Labeling scheme for the porphinato moiety.

Table IV. Important Internal Coordinates Contributing to the Potential Energy of Normal Modes above 1500 cm^{-1} in NiOEP (D_{4h})[a]

Symmetry	Obsd (CH_2Cl_2)	Internal coordinates
b_{1g}	1654	ν (C_a–C_m) >> ν (C_a–C_b) ~ δ (C_bC_aN) > ν (C_b–C_b)
a_{2g}	1603	ν (C_a–C_m) >> ν (C_a–N)
a_{1g}	1600	ν (C_b–C_b) >> ν (C_a–C_m) ~ δ (C_bC_aN)
b_{2g}(?)	1575	ν (C_a–N) > ν (C_a–C_m)
a_{1g}	1519	ν (C_a–N) > ν (C_a–C_m)

[a] Reference 28.

A striking effect of deuteration is the appearance of two additional anomalously polarized bands at 1263 and 1202 cm^{-1} (CH_2Cl_2) with a concurrent decrease in intensity of the 1310-cm^{-1} line. These bands are also observed in FeOEPCl-d_4 (Table II), and the 1202-cm^{-1} band in this complex has been reported by Kitagawa et al.[32] The reduced intensity of the unshifted 1310-cm^{-1} line relative to that of the 1395-cm^{-1} peak is not caused by NiOEP-h_4 which is present in less than 1% amount. It is possible that the 1 and 4% amounts of NiOEP-d_1 and -d_2, respectively, are responsible for the 1310-cm^{-1} line; however the shift to 1315 cm^{-1} in FeOEPCl-d_4 when compared to 1308 cm^{-1} FeOEPCl-h_4 implies that the weak anomalously polarized band is associated with the fully deuterated complexes. If this point is correct, then there are three anomalously polarized lines at 1395, 1310, and 1120 cm^{-1} which are not influenced appreciably by deuteration at the C_m carbon. It is generally agreed[28,32,33] that the contribution of δ (C_m–H) is greatest to the a_{2g} modes lying in the 1100–1500-cm^{-1} region; therefore, it is surprising to note that two or possibly three modes are altered slightly by deuteration.

In the low-frequency region of the spectrum, we cannot find persuasive evidence for metal–nitrogen stretching. The change in Ni–N bond length from 1.958 (2) Å[34] in the D_{4h} molecule to 1.929 (3) Å would be reflected in a frequency shift for this internal mode. An ir band at 348 cm^{-1} was suggested[29] as containing a Ni–N stretch contribution, but we find no shift in this frequency region for either the ir or resonance Raman spectrum when the two NiOEP crystal spectra are compared. Possibly the line at 225 cm^{-1} is shifted to 243 cm^{-1} as the Ni–N distance is decreased, but this line also moves upon deuteration. The difficulty in observing Ni–N frequencies in resonance Raman spectra is anticipated for these modes couple weakly with the $\pi^* \leftarrow \pi$ excitations.

Table V. Frequencies of Structure and Oxidation Sensitive Bands[a]

Compound	Distance from N plane	dp	$\bar{\nu}$, cm^{-1} ap	p	p	Bond length, Å C_a–C_m	C_a–N	Ref
$(FeOEP)_2O$	0.50	1630	1570	1494	1375	1.400 (10)	1.377 (8)	40
VOEtio	0.48	1635	1574	1500	1380	1.38 (2)	1.39 (2)	41
Fe^{III}ProtoDMECl	0.475	1634	1575	1496	1375	1.378 (17)	1.388 (19)	42
Fe^{III}OEPCl	0.455	1630	1568	1486	1378	1.377	1.395	43
ZnOEP	0.33	1622	1565	1493	1375	1.406 (2)	1.369 (2)	44
MgOEP	0.27	1610	1558	1482	1379	1.41 (1)	1.37 (1)	45
MnOEPCl	0.27	1642	1591[b]	1510	1379			46
Fe^{II}OEP(NO)	0.21	1648	1593	1514	1380	1.388 (4)	1.379 (3)	47
Co^{II}OEP(NO)	0.09	1656	1605	1521	1382	1.391 (3)	1.381 (4)	48
Co^{III}OEPBr[c]	?	1661	1579	1519	1380			
AgOEP	0	1601	1550	1482	1367			
$SnOEPCl_2$	0	1601	1545		1382	1.386 (5)	1.379 (5)	49
CuOEP	0	1638	1585	1505	1379	1.389 (4)	1.381 (10)	39
NiOEP (D_{2d})	0	1641	1590	1512	1382	1.372 (2)	1.386 (5)	12
RhEtio$(DMA)_2$Cl	0	1635	1578	1496	1382	1.39 (1)	1.37 (1)	50
NiOEP (D_{4h})	0	1660	1609	1524	1382	1.371 (4)	1.376 (6)	13
Fe^{III}OEP$(1m)_2$Cl	0	1643	1592	1509	1380	1.392 (9)	1.378 (8)	51
Fe^{II}Etio$(Py)_2$	0	1625	1587	1502	1367	1.369 (1)	1.384 (2)	52
Fe^{II}OEP(CO)(Py)	0	1636	1590	1503	1380			
Co^{III}OEP(OH)(Im)	~0	1649	1598	1514	1382			
$Co^{III}OEPClO_4$[c]	~0	1651	1598	1516	1386			
Co^{II}OEP[c]	~0	1651	1601	1515	1383			
Co^{II}OEP	~0	1655	1604	1518	1382			
Fe^{II}ProtoDME$(Py)_2$[c]	0	1623	1586	1496	1363			
Fe^{II}ProtoDME$(1m)_2$[c]	0	1624	1587	1495	1364			
Fe^{II}Proto$(1m)_2$[d]	0	1623	1587	1495	1362			
Fe^{II}Proto$(Py)_2$[d,e]	0	1624	1587	1497	1362			
Fe^{II}Proto$(CN)_2$[d]	0	1623	1590	1498	1363			
Fe^{III}Proto$(CN)_2$[d]	0	1639	1585	1509	1378			

[a] In KBr matrix. [b] Measured with 560.0-nm irradiation. [c] In CH_2Cl_2 solution. [d] In aqueous solution, pH 10.8. [e] In 3% SDS, pH 6.8.

We note that the solution spectrum of NiOEP is that of the D_{4h} planar form examined in the solid phase. [The frequency displacement (1–6 cm^{-1}) observed in CH_2Cl_2 is solvent-induced, since nickel etioporphyrin I which has a spectrum, above 1100 cm^{-1}, identical with the NiOEP D_{4h} form in the solid also exhibits (Figure 4) a slightly shifted spectrum when dissolved in CH_2Cl_2.] Thus, observation of the identical spectrum when the D_{2d} crystals are dissolved indicates the molecule, relieved of packing constraints and a neighboring nitromethane molecule, assumes a planar configuration: an experimental confirmation of the assumption by Hoard.[31]

When crystals of CuOEP evincing a spectrum containing depolarized bands at 1660 and 1638 cm^{-1} are dissolved, it is the molecular form whose spectrum displays the lower frequency line which is stable in solution. This behavior contrasts with the appearance of the high frequency 1654 (dp) cm^{-1} peak in solution spectra of planar NiOEP. Crystalline modifications of the free base of $\alpha,\beta,\gamma,\delta$-tetraphenylporphyrin are known; the triclinic form is approximately planar[35] while ruffling of the porphyrin is observed in the tetragonal form.[36] The $\alpha,\beta,\gamma,\delta$-tetraphenylporphyrin-copper(II) crystal is isomorphous[37] with the free base tetragonal form, suggesting that this metalloporphyrin is ruffled.[38] On the other hand, $\alpha,\beta,\gamma,\delta$-tetra($n$-propyl)porphyrincopper(II) is approximately planar.[39] Thus, the appearance of two molecular forms of CuOEP as inferred from the resonance Raman data is quite reasonable. X-Ray structural determination of CuOEP would be quite interesting, inasmuch as analogy with the NiOEP example would imply that the ruffled form of the copper complex is stable in solution; nonetheless, we assign the solution spectrum to a planar form, there being no apparent reason for the retention of a ruffled core in solution.[31]

Structural Implication. Collected in Table V are frequencies observed in metalloporphyrins of both the structure-sensitive bands and the 1380 (p) cm^{-1} line advanced as an oxidation state marker in hemeproteins.[1,5] Listed also is the distance from the metal to the basal nitrogen plane; the distance d(Ct–M) will be referred to in subsequent discussions of out-of-plane displacement of metal atoms. Structural parameters are generally obtained from metallotetraphenylporphyrin data. In view of the lengthening[49] of the metal to C_m distance upon meso substitution, bond lengths only are meant to be indicative when applied to MOEP complexes.

Examination of the Raman data shows that the difference between the highest frequency depolarized and anomalously polarized lines is relatively constant at 54 ± 4 cm^{-1} excepting values from Co^{III}OEPBr and iron(II) complexes. The constancy reflects the large and almost equal contributions of ν (C_a–C_m) to the two modes. Also, excepting AgOEP and iron(II) complexes, the 1380 (p) cm^{-1} line is remarkably insensitive to the central metal. In the cited complexes the polarized line is at 1364–1367 cm^{-1}, a frequency region observed earlier[1] for ferrocytochrome c (1362 cm^{-1}) and deoxyhemoglobin (1358 cm^{-1}). There is no specific environmental influence on this polarized line since solid, CH_2Cl_2, or aqueous solution samples of the low-spin iron(II) compounds exhibit the 1364–1367-cm^{-1} frequency. In view of anticipated differences in charge density migration from the various metal ions to the porphyrin skeleton and in view of the invariance of the 1380-cm^{-1} value obtained with the metal ions examined here, it appears that the charge distribution about the iron(II) atom is not the fundamental factor in positioning this line.

We have suggested earlier that when the a_{2g} frequency was greater than 1580 cm^{-1}, the metal was in-plane. The larger set of resonance Raman and structural data now available shows some striking exceptions: $SnOEPCl_2$ (1545 cm^{-1}) and AgOEP (1550 cm^{-1}) are known to be in-plane; yet, the suggested resonance Raman classification would assign them as out-of-plane. The quantitive utility of the

aforementioned classification leaves much to be desired when FeOEP(NO) (1593 cm^{-1}) is assigned as in-plane; yet, a recent structural analysis[47] shows the iron to be displaced from the plane by 0.21 Å in FeTPP(NO). Finally, the mechanism by which displacement of the metal could induce changes in the vibrational frequencies of the porphyrin skeleton is unknown. Spiro and Strekas[1] have suggested that doming of the porphyrin ring accompanying metal displacement partially interrupted π conjugation in the porphyrin skeleton; in turn, this interruption influenced positions of the structure-sensitive bands. Some support for this notion is found in NiOEP complexes in which severe S_4 ruffling of the D_{2d} form causes a shift to lower frequency. However, the $SnOEPCl_2$ (1545 cm^{-1}) and D_{4h} NiOEP (1609 cm^{-1}) data would seem to obviate this mechanism for the majority of complexes, since both molecules are planar. Fortunately, the outlook for a structural application of resonance Raman data is not as pessimistic as the above examples indicate; we have noticed that the a_{2g} frequency correlates remarkably well with d(Ct-N), the distance between the center of the porphyrin core and the pyrrole nitrogen (Figure 5).

In Table VI the metalloporphyrins are listed in order of decreasing Ct-N distance. The correspondence between a decrease in this distance and an increase in the a_{2g} frequency is apparent; the correlation is far superior to any casual relation between individual (or collections of) bond lengths and frequency. We note that in the rhodium complex the peak position is ~10 cm^{-1} higher than might be expected on the basis of its Ct-N distance and the NiOEP (D_{2d}) complex displays its perversity by decreasing its frequency to 1590 cm^{-1} although the critical distance shortens. It is likely in this specific case that the severe S_4 ruffling, in releasing strain in the porphyrin, assumes a role in determining the frequency shift. However, in the remainder of the metalloporphyrins distortion of the macrocycle is not severe, and we advance the following mechanism to account for the change in the a_{2g} frequency with d(Ct-N). If d(Ct-N) is a measure of the radius of the inner 16-membered ring, then expansion of the ring with retention of the pyrrole unit geometry will increase $d(C_a-C_m)$ and the $C_a-C_m-C_a$ angle. In this simple picture, the π-bond order between C_a and C_m atoms decreases and contributes to a lowering of structure-sensitive frequencies. Pariser-Parr-Pople self-consistent calculations on NiOEP (D_{4h}) and $SnOEPCl_2$, utilizing the averaged geometry of the complexes,[13] confirm the π-bond order decrease in the tin compound.

The empirical relation noted between d(Ct-N) and the anomalously polarized frequency suggests assessment of the out-of-plane excursion of the metal is possible, if the metal-to-pyrrole nitrogen distance, d(M-N), can be estimated. Since d(Ct-N), d(M-N) $\gg$ d(Ct-M), errors in the former lengths will induce relatively large errors in d(Ct-M). For example, when d(Ct-N) = 2.00 (1) Å and d(M-N) = 2.05 (1) Å, d(Ct-M) is calculated to be 0.45 (9) Å. Nonetheless, it is of interest to examine predictions of this correlation as applied to hemeprotein data.

In the case of oxyhemoglobin d(Fe-N) = 2.00 Å is anticipated for a low-spin iron(II) complex. The anomalously polarized line of oxyhemoglobin appears[1] at 1585 cm^{-1} which matches well the 1587-cm^{-1} value found for bis(imidazole)protoporphyrin IX iron(II) in water and its dimethyl ester in CH_2Cl_2. The value of d(Ct-N) so implied is 2.00 Å, and the conclusion that oxyhemoglobin contains in-plane iron is well known.[54,55]

More interesting is an assessment of iron displacement in deoxyhemoglobin. The anomalously polarized line appears[1] in the spectrum at 1552 cm^{-1}. Adjustment of this frequency by addition of ~4 cm^{-1} is required when comparison of frequencies taken with solid samples is made with those in solution. Thus D_{4h} NiOEP (crystal) exhibits an anomalously polarized line at 1609 cm^{-1} while in solution the band is located at 1603 cm^{-1}. Also, the spectrum of protoporphyrin IX dimethyl ester iron(III) chloride displays the line at 1574 and 1570 cm^{-1}, respectively, in solid and solution samples. The corrected value of 1556 cm^{-1} in deoxyhemoglobin is close to the 1558-cm^{-1} band found with MgOEP, and we interpret the Raman data as indicating an expansion of the core to d(Ct-N) = 2.05 (1) Å. Hoard had tentatively suggested[54] a d(Fe-N) of 2.14 Å was appropriate to high-spin iron(II), but a structural determination of (1-methylimidazole)-tetraphenylporphinatoiron(II) yields d(Fe-N) of 2.086 Å.[56] Upon setting d(Fe-N) at 2.086 Å, a Ct-Fe displacement of 0.39 (6) Å is obtained for the iron in deoxyhemoglobin; a value in good agreement with the 0.42-Å displacement found in the model high-spin iron(II) porphyrin and well below the estimated 0.70-0.83 Å advanced by Perutz.[57]

Consideration of oxy- and deoxycoboglobin for which anomalously polarized bands are observed[58] at 1596 and 1593 cm^{-1}, respectively, yields a Ct-N distance of 1.98-1.99 Å. With reported Co(II)-N distances of 1.96 (1) and 1.977 (3) Å or a Co(III)-N length of 1.978 (5) Å in model complexes, the resonance Raman data would suggest only slight movement of the cobalt atom upon binding of oxygen. In both forms of coboglobin, the metal is close to being in-plane. We cannot determine if the displacement is as great as the maximum value of 0.15 Å suggested earlier[58] due to the geometrical problem in calculating small out-of-plane displacements.

Application of the method to fluoromethemoglobin[1] [1555 (ap) cm^{-1}] with d(Fe-N) = 2.07 (1) Å[54] yields an out-of-plane displacement of 0.3 (1) Å, a value ~0.1 Å less than found here in deoxyhemoglobin, 0.2 Å less than observed in model high-spin ferric complexes, but in agreement with the published estimate of 0.3 Å.[59] As found with deoxyhemoglobin there is inferred a curious expansion of the core region not observed in model high-spin ferric compounds.

Spiro[1,3] has suggested that doming of the porphyrin ring will lower the structure-sensitive frequencies, and the low frequencies observed at ~1555 (ap) cm^{-1} in high-spin iron-

Table VI. Correlation of the Anomalously Polarized Frequency with Ct-N Distance[a]

Compound	$\bar{\nu}$, cm^{-1}	Ct-N, Å	Structure	Ref
$SnOEPCl_2$	1545	2.082 (2)	$SnOEPCl_2$	49
AgOEP	1550	~2.08	AgTPP	53
MgOEP	1558	2.055 (6)	$MgTPP(H_2O)$	45
ZnOEP	1565	2.047 (2)	PyZnTPyP	44
RhEtio$(DMA)_2Cl$	1578	2.038 (6)	RhEtio$(DMA)_2Cl$	50
$(FeOEP)_2O$	1570	2.027	$(FeTPP)_2O$	40
FeOEPCl	1568	2.019 (3)	Average hemin	54
FeProtoDMECl	1575	2.007 (5)	FeProtoCl	42
VOEtio	1574	2.01 (4)	VODPEP	41
PdOEP	1585	2.009 (9)	PdTPP	32, 37
Fe^{II}Etio$(Py)_2$	1587	2.004 (4)	$Fe^{II}TPP(Im)_2$	52
CuOEP	1585	2.000 (5)	CuTPrP	39
$Fe^{III}OEP(Im)_2Cl$	1590	1.989 (5)	$Fe^{III}TPP(Im)_2Cl$	51
FeOEP(NO)	1593	1.990	FeTPP(NO)	47
MnOEPCl	1591	1.99	MnTPPCl	46
CuOEP	1605	1.981 (7)	CuTPP	37
CoOEP(NO)	1605	1.976 (3)	CoTPP(NO)	48
NiOEP (D_{4h})	1609	1.958 (2)	NiOEP	13
NiOEP (D_{2d})	1590	1.929 (3)	NiOEP	12

[a] Abreviations: Py = pyridine, Im = imidazole, TPyP = tetra(4-pyridyl)porphinato, DMA = dimethylamine, Proto = protoporphyrin IX, DPEP = deoxyphylloerythroetioporphinato, TPrP = tetra(*n*-propyl)porphinato, DME = dimethoxy ester.

(II) or iron(III) hemeproteins result from doming due to out-of-plane displacement of the metal. Doming is defined by Hoard[31] as the symmetric movement of pyrrole nitrogen atoms upward from the mean porphyrin plane toward the five-coordinate metal atom. An additional protein-induced doming of the porphyrin is advanced by Hoard and Scheidt[56] and critically assessed by Little and Ibers.[60] By contrast, the point of view advanced here, while not disproving the doming mechanism, suggests that the well-documented expansion of the porphinato core will induce shifts in structure-sensitive bands via changes of the force constants associated with internal coordinates of atoms comprising the 16-membered ring.

The structural implication of the two interpretations differs when the anomalously polarized line is lower than ~1580 cm^{-1}. Since doming is primarily a result of metal displacement from the porphyrin plane, this mechanism would indicate that high-spin ferric hemeproteins such as methemoglobin fluoride or horseradish peroxidase fluoride possess the *maximum* extension of d(Ct–Fe). To account for the difference between the 1570-cm^{-1} position found for FeOEPCl and the cited value of 1555 cm^{-1} in hemeproteins, an additional protein-induced doming is required. In contradistinction, we interpret the 1555-cm^{-1} line as indicating an increase in d(Ct–N) and, with a fixed value of d(Fe–N), a *decrease* in d(Ct–Fe). Thus, d(Ct–Fe) is ~0.3–0.4 Å in high-spin ferric hemeproteins. It is possible to envisage that axial ligands occupying the distal position will pull the six-coordinate metal toward the porphyrin plane.

It is noted that a moderate decrease of d(Ct–Fe) from the 0.5-Å value in model complexes is not inconsistent with retention of high-spin magnetic properties which are more sensitive to rhombic distortions in the crystal field than to the value of d(Ct–Fe).[61,62] For example, the spectrum of horseradish peroxidase fluoride possesses a band at 1555 cm^{-1} while the benzhydroxamic acid derivative exhibits a line at 1566 cm^{-1}; both hemeproteins are high spin (μ_{eff} = 5.90–5.92 μ_B) and involve modifications in the distal region.[63,64] These observations are not readily accommodated by doming if one ascribes a larger d(Ct–Fe) value to the fluoride complex and concurrently argues that the magnetic moment is a faithful representation of this distance. Instead, we interpret the data as indicating a larger d(Ct–N) value for the fluoride complex and, since d(Fe–N) is presumed invariant in the two high-spin complexes, a smaller Ct–Fe distance in horseradish peroxidase fluoride.

At pH 7 native horseradish peroxidase has an anomalously polarized line at 1574 cm^{-1} and a magnetic moment of 5.2 μ_B,[63,64] a value which reflects an increased rhombic component in the crystal field as compared with the benzhydroxamic acid derivative. The doming model[65] would ascribe a more planar porphyrin core and smaller iron out-of-plane displacement to the native enzyme than the peroxidase complexes discussed above. Alternatively, the 1574-cm^{-1} value is characteristic of model high-spin ferric complexes listed in Table VI and we suggest ~0.5 Å is the extent of metal displacement. This example demonstrates that the structural interpretation of Raman data we favor may yield an increased Ct–Fe distance in a hemeprotein with a reduced magnetic moment.

It is doubtful if arbitrary adjustment of the force field and the calculated normal mode frequencies so as to simulate doming or core expansion will prove definitive in excluding one or the other mechanism; indeed, both may be operative. An experimental approach is desirable. For example, systematic studies of the magnetic, Raman, and crystallographic properties of a model ferric porphyrin containing one covalently linked imidazole should be illuminating. Upon variation of the counterion or sixth ligand it may be feasible to change the Ct–Fe distance by 0.1–0.2 Å without inducing concomitant alterations in doming.

Acknowledgment. We wish to express our appreciation to Drs. J. H. Fuhrhop, M. Gouterman, L. Hanson, and D. Dolphin for supplying porphyrin samples and to Professor Kyogoku for allowing citation of his normal mode results prior to publication. This research was supported in part by grants from the National Institutes of Health (GM-18894 and AM-14344), the National Science Foundation (GP-17061), and the Research Corporation. L. D. Spaulding was a National Institutes of Health Postdoctoral Fellow.

References and Notes

(1) T. G. Spiro and T. C. Strekas, *J. Am. Chem. Soc.*, **96**, 338 (1974).
(2) H. Sussner, A. Mayer, and H. Brunner, *Eur. J. Biochem.*, **41**, 465 (1974).
(3) T. G. Spiro, *Acc. Chem. Res.*, **7**, 339 (1974).
(4) L. A. Nafie, M. Pezolet, and W. L. Peticolas, *Chem. Phys. Lett.*, **20**, 563 (1973).
(5) T. Yamamoto, G. Palmer, D. Gill, I. T. Salmeen, and L. Rimai, *J. Biol. Chem.*, **284**, 5211 (1973).
(6) T. M. Loehr and J. S. Loehr, *Biochem. Biophys. Res. Commun.*, **55**, 218 (1973).
(7) K. N. Solovyov, N. M. Ksenofontova, S. F. Shkirman, and T. F. Kachura, *Spectrosc. Lett.*, **6**, 455 (1973).
(8) H. Burger, K. Burczyk, J. W. Buchler, J. H. Fuhrhop, F. Hofler, and B. Schrader, *Inorg. Nucl. Chem. Lett.*, **6**, 171 (1970).
(9) A. L. Verma and H. J. Bernstein, *Biochem. Biophys. Res. Commun.*, **57**, 255 (1974).
(10) A. L. Verma, R. Mendelsohn, and H. J. Bernstein, *J. Chem. Phys.*, **61**, 383 (1974).
(11) R. H. Felton, N. T. Yu, D. C. O'Shea, and J. A. Shelnutt, *J. Am. Chem. Soc.*, **96**, 3675 (1974).
(12) E. F. Meyer, Jr., *Acta Crystallogr., Sect. B*, **28**, 2162 (1972).
(13) D. L. Cullen and E. F. Meyer, Jr., *J. Am. Chem. Soc.*, **96**, 2095 (1974).
(14) A. D. Adler, F. R. Longo, F. Kampas, and J. Kim, *J. Inorg. Nucl. Chem.*, **32**, 2443 (1970).
(15) M. Gouterman, F. P. Schwartz, P. D. Smith, and D. Dolphin, *J. Chem. Phys.*, **59**, 679 (1973).
(16) J. H. Fuhrhop and D. Mauzerall, *J. Am. Chem. Soc.*, **91**, 4174 (1969).
(17) W. S. Caughey, C. H. Barlow, D. H. O'Keeffe, and M. C. O'Toole, *Ann. N.Y. Acad. Sci.*, **206**, 296 (1973).
(18) J. E. Falk, "Porphyrins and Metalloporphyrins", Elsevier, New York, N.Y., 1964.
(19) H. Kobayashi and Y. Yanagawa, *Bull. Chem. Soc. Jpn.*, **45**, 450 (1972).
(20) D. Dolphin, A. Forman, D. C. Borg, J. Fajer, and R. H. Felton, *Proc. Natl. Acad. Sci. U.S.A.*, **68**, 614 (1971).
(21) R. Bonnett and G. S. Stephenson, *Proc. Chem. Soc., London*, 291 (1964).
(22) W. L. Peticolas, L. Nafie, P. Stein, and B. Fanconi, *J. Chem. Phys.*, **52**, 1576 (1970).
(23) M. Gouterman in "Excited States of Matter", C. W. Shoppe, Ed., Graduate Studies, Texas Tech University, 1973, pp 63–103.
(24) T. C. Strekas and T. G. Spiro, *J. Raman Spectrosc.*, **1**, 387 (1973).
(25) W. M. McClain, *J. Chem. Phys.*, **55**, 2789 (1971).
(26) M. Pezolet, L. A. Nafie, and W. L. Peticolas, *J. Raman Spectrosc.*, **1**, 455 (1973).
(27) D. W. Collins, D. B. Fitchen, and A. Lewis, *J. Chem. Phys.*, **59**, 5714 (1973).
(28) M. Abe, T. Kitagawa, and Y. Kyogoku, private communication.
(29) H. Ogoshi, Y. Saito, and K. Nakamoto, *J. Chem. Phys.*, **57**, 4194 (1972).
(30) M. Gouterman, *J. Mol. Spectrosc.*, **6**, 138 (1961).
(31) J. L. Hoard, *Ann. N.Y. Acad. Sci.*, **206**, 18 (1973).
(32) T. Kitagawa, H. Ogoshi, E. Watanabe, and Z. Yoshida, *Chem. Phys. Lett.*, **30**, 451 (1975).
(33) R. Mendelsohn, S. Sunder, A. L. Verma, and H. J. Bernstein, *J. Chem. Phys.*, **62**, 37 (1975).
(34) Values in parentheses are estimated standard deviations of least significant figures.
(35) S. Silvers and A. Tulinsky, *J. Am. Chem. Soc.*, **89**, 3331 (1967).
(36) M. J. Harmor, T. A. Harmor, and J. L. Hoard, *J. Am. Chem. Soc.*, **86**, 1938 (1964).
(37) E. B. Fleischer, C. Miller, and L. Webb, *J. Am. Chem. Soc.*, **86**, 2342 (1964).
(38) E. B. Fleischer, *J. Am. Chem. Soc.*, **85**, 1353 (1963).
(39) I. Moustakali and A. Tulinsky, *J. Am. Chem. Soc.*, **95**, 6811 (1973).
(40) A. B. Hoffman, D. M. Collins, V. W. Day, E. B. Fleischer, T. S. Srivastava, and J. L. Hoard, *J. Am. Chem. Soc.*, **94**, 3620 (1972).
(41) R. C. Peterson, *Acta Crystallogr., Sect. B*, **25**, 2527 (1969).
(42) D. F. Koenig, *Acta Crystallogr.*, **18**, 663 (1965).
(43) J. L. Hoard, M. J. Harmor, T. A. Harmor, and W. S. Caughey, *J. Am. Chem.Soc.*, **87**, 2312 (1965).
(44) D. M. Collins and J. L. Hoard, *J. Am. Chem. Soc.*, **92**, 3761 (1970).
(45) R. Timkovich and A. Tulinsky, *J. Am. Chem. Soc.*, **91**, 4430 (1969).
(46) L. J. Boucher, *Coord. Chem. Rev.*, **7**, 289 (1972), references unpublished data of B. M. Chen and A. Tulinsky.
(47) W. R. Scheidt and M. E. Frisse, *J. Am. Chem. Soc.*, **97**, 17 (1975).
(48) W. R. Scheidt and J. L. Hoard, *J. Am. Chem. Soc.*, **95**, 8281 (1973).
(49) D. L. Cullen and E. F. Meyer, Jr., *Acta Crystallogr., Sect. B*, **29**, 2507

(1973).
(50) L. K. Hanson, M. Gouterman, and J. C. Hanson, *J. Am. Chem. Soc.*, **95**, 4822 (1973).
(51) R. Countryman, D. M. Collins, and J. L. Hoard, *J. Am. Chem. Soc.*, **91**, 5166 (1969).
(52) L. J. Randonovich, A. Bloom, and J. L. Hoard, *J. Am. Chem. Soc.*, **94**, 2073 (1972).
(53) See discussion following A. Tulinsky, *Ann. N.Y. Acad. Sci.*, **206**, 47 (1973).
(54) J. L. Hoard, *Science*, **174**, 1295 (1971).
(55) J. P. Collman, R. R. Gagne, C. A. Reed, W. T. Robinson, and G. A. Rodley, *Proc. Natl. Acad. Sci. U.S.A.*, **71**, 1326 (1974).
(56) J. L. Hoard and W. R. Scheidt, *Proc. Natl. Acad. Sci. U.S.A.*, 70, 3919 (1973).
(57) M. F. Perutz, *Nature (London)*, **237**, 995 (1972).
(58) W. H. Woodruff, T. G. Spiro, and T. Yonetani, *Proc. Natl. Acad. Sci. U.S.A.*, **71**, 1065 (1974).
(59) M. Perutz, *Nature (London)*, **228**, 726, 734 (1970).
(60) R. G. Little and J. A. Ibers, *J. Am. Chem. Soc.*, **96**, 4452 (1974).
(61) D. W. Smith and R. J. P. Williams, *Struct. Bonding (Berlin)*, **7**, 1 (1970).
(62) J. M. Rifkind in "Inorganic Biochemistry", Vol. 2, G. L. Eichhorn, Ed., Elsevier, New York, N.Y., 1973, p 832.
(63) G. R. Schonbaum, A. Romans, R. Felton, and N. T. Yu, unpublished data.
(64) G. R. Schonbaum, *J. Biol. Chem.*, **248**, 502 (1973).
(65) G. Rakshit and T. G. Spiro, *Biochemistry*, **13**, 5317 (1974).

Molecular and Crystal Structure of Streptonigrin

Yuan-Yuan H. Chiu and William N. Lipscomb*

Contribution from the Gibbs Chemical Laboratory, Harvard University, Cambridge, Massachusetts 02138. *Received August 16, 1974*

Abstract: The chemical structure assigned by Rao, Biemann, and Woodward is confirmed in an X-ray diffraction study of streptonigrin cocrystallized with ethyl acetate. Rings A, B, and C, including the carboxyl group on ring C, are very nearly coplanar. This configuration is partially maintained by a short, probably bent, hydrogen bond (2.65 Å) between the NH_2 of ring C and the N atom within ring B. The space group is $P2_12_12_1$, and there are four molecules of streptonigrin and four molecules of ethyl acetate in a unit cell having dimensions $a = 13.676$, $b = 30.663$, and $c = 6.821$ Å. For the 1677 independent X-ray diffraction maxima the value of $R = \sum||F_o| - |F_c||/\sum|F_o|$ is 0.098.

Streptonigrin, isolated by Rao and Cullen[1] as a metabolite of streptomyces flocculus, is an antibiotic. Showing activity against tumor,[2-4] against lymphoma,[5] and also against several viruses,[6] streptonigrin has a number of undesirable side effects[3] including severe bone marrow depression, nausea, vomiting, diarrhea, and alopecia. It causes chromosomal damage[7,8] when added to cultures of human leucocytes, inhibits DNA synthesis in tissue culture cells[9-11] and in bacteria,[9,12-14] and inhibits partial RNA and protein synthesis.[9] Streptonigrin also causes single strand breaks[7,8] on DNA upon reduction and subsequent reaction with oxygen.[14] At least two types of binding, reversible and irreversible (upon dialysis), occur when streptonigrin interacts with calf thymus DNA.[13] Reduction of streptonigrin is not required for binding, and association appears to occur primarily with the dCMP portion of DNA.

The bacteriocidal activity of streptonigrin is similar to that of mitomycin which also has an aminoquinone fragment,[15] a structural feature common to several closely related antitumor agents.[15,16] The possibility that the semiquinone form of streptonigrin is involved in its activity has been examined by electron spin resonance methods.[10,17,18]

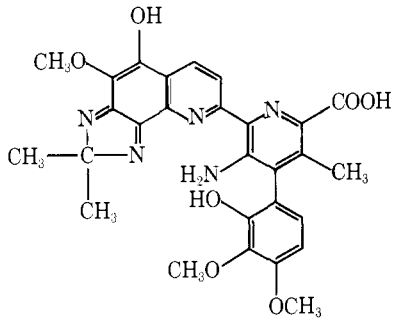

A derivative, isopropylidene azastreptonigrin, has significant antitumor activity in animals only at 100 times the normal dosages of streptonigrin.[19] Even at 10^5 times the dosages, there is no antibactericidal effect or cytotoxicity in tissue cultures, no effect on DNA synthesis, and no activity against virus.[6,20] It also lacks the reduction and subsequent oxygenation reactions of streptonigrin, thus demonstrating the critical nature of the aminoquinone function region of streptonigrin.[19] Moreover, since the methyl ester of streptonigrin has $^1/_{100}$th the activity of streptonigrin in tissue culture cells,[20] $^1/_{500}$th the activity against Meloney leukemia virus replication, and $^1/_3$rd the activity in inhibiting the DNA polymerase of C-type RNA virus,[6] the carboxyl group probably is another chemical or stereochemical site of interest.

We report a crystal structure study of streptonigrin in which the aminoquinone function is intact. The three-dimensional ring orientations may be of value in elucidating its interactions with DNA or RNA, and may aid in interpreting later steps in its complex sequence of reactions in bacteria and in tumors.

Structure Determination. Fragile, dark brown, thick plates were grown as single crystals of streptonigrin cocrystallized with the solvent, ethyl acetate. The crystal data are given in Table I. The unit cell dimensions were determined from Weissenberg photographs on which Al powder diffraction lines were superimposed. Their values and errors were obtained by least squares by minimizing

$$\sum_{n=1}^{N} w_n(\sin^2 \theta_{obsd} - \sin^2 \theta_{calcd})^2$$

where the weights w_n are $1/\sin^2 \theta_{obsd}$, and $N = 41$ reflections. The experimental density was determined by suspension in a solution of *n*-heptane and carbon tetrachloride (Table I). Omission of the four ethyl acetate molecules led to an unreasonably low calculated density of 1.182 g/cm^3.

The structure was eventually solved from data taken from multiple level Weissenberg photographs of one crystal mounted about *c* (hkL for $0 \leq L \leq 5$) and a second crystal mounted about *a* (Hkl for $0 \leq H \leq 5$), using Cu Kα radiation which had been filtered through Ni foil. Aside from the extremely intense 002 and 022 reflections (>300), which